Subgap structure in asymmetric superconducting tunnel junctions

Markus Ternes,[1,*] Wolf-Dieter Schneider,[1] Juan-Carlos Cuevas,[2] Christopher P. Lutz,[3]
Cyrus F. Hirjibehedin,[3] and Andreas J. Heinrich[3]
[1]*Institut de Physique des Nanostructures, École Polytechnique Fédérale de Lausanne, CH-1015 Lausanne, Switzerland*
[2]*Institut für Theoretische Festkörperphysik, Universität Karlsruhe, D-76128 Karlsruhe, Germany*
[3]*IBM Research Division, Almaden Research Center, 650 Harry Road, San Jose, California 95120, USA*
(Received 13 September 2005; published 2 October 2006)

Conductance measurements between two superconducting electrodes with different gap energies Δ_1 and Δ_2 were performed with a low-temperature scanning tunneling microscope. The temperature dependence and tip-sample distance dependence of the spectra show a pronounced subgap structure which is interpreted as multiple Andreev reflections (MARs). Low temperature conductance peaks not seen in symmetric superconducting tunnel junctions arise at energies $\pm|\Delta_1-\Delta_2|$ when the superconducting gaps are sufficiently different. We propose an explanation of these findings by extending the full counting statistics of MARs to describe these asymmetric junctions.

DOI: 10.1103/PhysRevB.74.132501 PACS number(s): 74.45.+c, 68.37.Ef, 74.50.+r

For more than 40 years the subgap structure of superconducting-insulating-superconducting (*SIS*) junctions has been in the focus of experimental and theoretical investigations.[1,2] In these systems the transport is dominated by multiple Andreev reflections.[3] These tunneling processes have emerged as a key concept in superconductivity mainly due to recent break-junction experiments.[4–7] In these experiments the coupling between the superconductors is varied continuously, a necessity for a thorough understanding of Andreev reflections[8,9] and Josephson supercurrent.[10]

Asymmetric junctions are an unexplored regime in the current framework of Andreev reflections. Because the degeneracy of the gap energies is broken, these systems are predicted to show new spectroscopic features due to the loss and the opening of new Andreev reflection processes.[11] Experimental studies of Andreev reflections in asymmetric tunnel junctions would therefore provide crucial insight into subgap processes in *SIS* systems.

It is possible to study asymmetric tunnel junctions with a scanning tunneling microscope (STM) because the tip and sample can have different gap energies.[12] This contrasts with current break-junction techniques, in which the gap energies must be equal. The coupling between the superconductors in STM junctions can be varied by changing the tip-sample distance.[13,14] So far, however, Andreev reflections have been detected only in symmetric STM junctions.[15]

Here we present an experimental study of the subgap structure of asymmetric *SIS* tunnel junctions. We use a procedure to create the asymmetric *SIS* junction in an STM by attaching a superconducting microcrystal to a normal conducting tip. Due to finite size effects,[16,17] the energy gap of the microcrystal is reduced with respect to the bulk sample value. This technique is particularly powerful because it enables us to vary the asymmetry of the junction by simply using different microcrystals.

In asymmetric niobium junctions created with this technique, we find peaks in the conductance spectra at energies of $\pm|\Delta_1-\Delta_2|$ at low temperatures. These new features arise at low junction resistances when the difference between Δ_1 and Δ_2 is sufficiently large. This surprising spectral feature is explained by extending the framework of Andreev scattering and the concept of full counting statistics[18] to include the asymmetry of the gap energies. The applicability of the MAR model in the asymmetric regime lends strong support to its validity.

The measurements were performed using an STM under UHV conditions in a ^{3}He Joule-Thomson refrigerator.[19] We used a Nb(110) single crystal sample which was cleaned by successive cycles of heating and Ar-ion sputtering until we resolved a flat surface.[20] The superconducting gap of the sample $\Delta_1=1.47$ meV was probed using a cut Ir wire as normal conducting tip. By indenting the Ir tip into the Nb sample we attached a Nb microcrystal on the apex of the tip resulting in a superconducting gap Δ_2 ranging from 21–86 % of the bulk Nb value. Using these tips and the Nb(110) sample we performed conductance (dI/dV) measurements by modulating the junction voltage with a small sinusoidal voltage $V_{\mathrm{mod}}=10\ \mu V_{\mathrm{r.m.s}}$ and detecting the signal with standard lock-in technique.

Figure 1 shows a set of dI/dV measurements using a tip with a superconducting gap of $\Delta_2=1.27$ meV at $T=0.56$ K and different values of the nominal junction resistance R which were determined outside the gap at $V=5$ mV. By successively reducing the resistance and thereby increasing the coupling between the two superconductors, we observe the evolution of subgap conductance peaks at characteristic energies of $\pm\Delta_1$, $\pm\Delta_2$, and $\pm(\Delta_1+\Delta_2)/3$. Also observed is the peak at $V=0$ corresponding to the Josephson supercurrent. These are observations of MAR in asymmetric superconducting tunnel junctions, which are predicted to occur at energies $\pm\Delta_1/m$, $\pm\Delta_2/m$, and $\pm(\Delta_1+\Delta_2)/(2m+1)$, where m is an integer.[11] Processes involving one and two Andreev reflections representing the observed subgap peaks are shown schematically in Fig. 4(a)(i–iii).

The subgap structure observed in Fig. 2 for a tip with a gap $\Delta_2=0.32\ \mathrm{meV}\approx 0.21\times\Delta_1$ is substantially different. While the peaks at $\pm\Delta_1$ and $\pm\Delta_2$ are still present, the peaks at $\pm(\Delta_1+\Delta_2)/3$ are only faintly visible. Surprisingly, peaks at $\pm(\Delta_1-\Delta_2)$, corresponding to ± 1.15 meV, appear at lower junction resistances. These features are not present in junc-

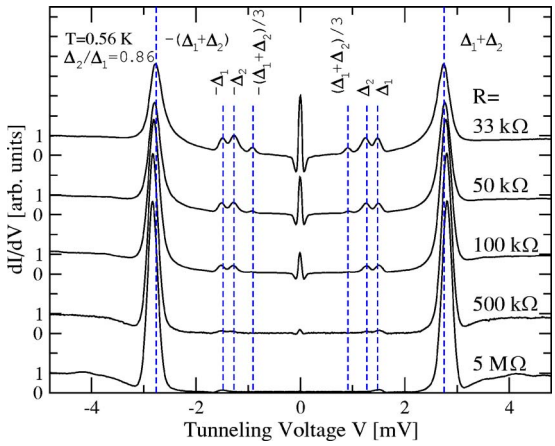

FIG. 1. (Color online) dI/dV spectra observed at 0.56 K between a superconducting sample and tip with nearly equal gaps (Δ_1=1.47 meV, Δ_2=1.27 meV) showing Andreev reflections for different junction resistances. All spectra are normalized by R. The peak evolving at V=0 is due to the Josephson supercurrent. The dotted lines are a guide for the eye marking characteristic features in the spectra. The spectra are shifted vertically with respect to each other for better visibility.

tions with nearly equal gaps shown in Fig. 1. Notice that $eV=\Delta_1-\Delta_2$ does not correspond to the threshold voltage of any predicted MAR process.[11]

To clarify the origin of this novel spectral feature, we measured the temperature dependence at constant junction resistance, which is shown in Fig. 3(a). As the temperature increases all features smear out and the supercurrent peak as well as the peaks at Δ_1 and Δ_2 diminish. Above approxi-

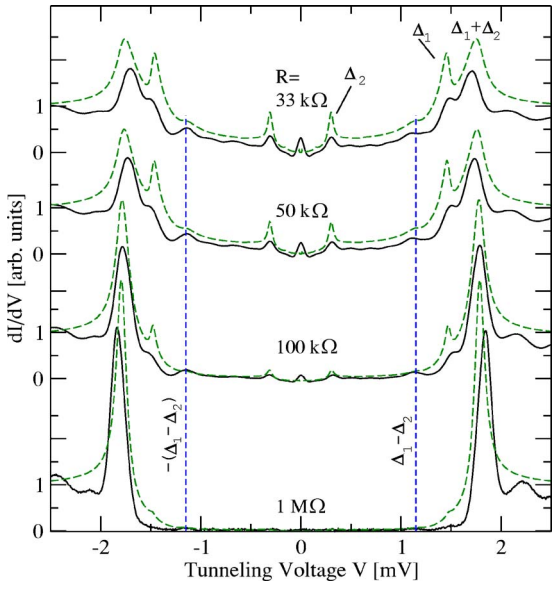

FIG. 2. (Color online) Full lines: dI/dV spectra measured between a Nb sample (Δ_1=1.47 meV) and a tip with a small gap (Δ_2=0.32 meV) at 0.56 K and different junction resistances. All spectra are normalized by R. Dashed lines: Results of the single-channel MAR theory of Ref. 9. The transmission coefficient τ is determined by the corresponding R. Vertical lines: A guide for the eye to mark a new feature at $\pm(\Delta_1-\Delta_2)$.

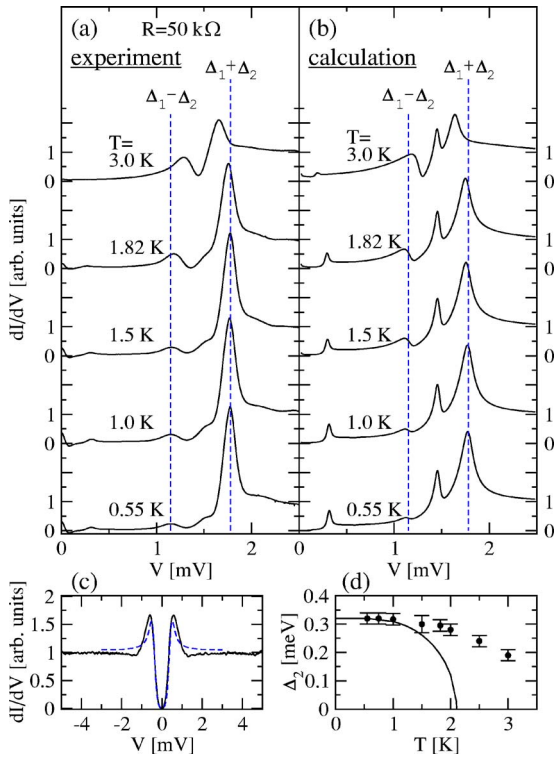

FIG. 3. (Color online) (a) Temperature dependent dI/dV spectra observed at R=50 kΩ between tip and sample as in Fig. 2. All spectra are normalized by R. (b) Results of the MAR theory with τ=0.26. Vertical lines: A guide for the eye marking the $\Delta_1\pm\Delta_2$ positions at 0 K. (c) Spectrum of a typical superconducting tip measured against a normal conducting Cu(111) sample at 0.56 K with V_{mod}=50 $\mu V_{\mathrm{r.m.s.}}$ and R=5 MΩ (full line) and BCS calculation using Δ=0.41 meV and T=0.6 K (dashed line). (d) Dots: Temperature dependence of the superconducting tip gap Δ_2 for the tip shown in (a). Full line: BCS calculation.

mately 1.5 K, the height of the peak at $\Delta_1-\Delta_2$ increases significantly due to thermally activated tunneling of single quasiparticles,[21] while below 1.5 K the intensity of the peak stays constant indicating that at low temperatures the peak is not due to thermal excitation of quasiparticles.[23]

The structure of the dI/dV spectrum with the characteristic peak at $eV=\Delta_1+\Delta_2$ is still visible at a temperature of 3 K. This is well above the critical temperature of T_C=2.1 K expected for a BCS superconductor with Δ=0.32 meV. Figure 3(d) shows the unusual behavior of $\Delta_2(T)$, which is presumably due to the small size of the microcrystal.[22] Here Δ_2 was obtained by fitting dI/dV spectra of the tips, measured against a Cu(111) sample, by assuming a bulk BCS density of states for the tip. As seen in Fig. 3(c), such fits reproduce the gap structure of the spectra very well, but have noticeable differences in the tails of the line shape.

To interpret the observed peak structure, we apply a version of the single-channel MAR theory of Ref. 9. We have calculated the conductance for various temperatures and junction resistances[24] by using bulk BCS density of states for the sample and tip with the measured gaps Δ_1 and Δ_2. As seen in Fig. 2, MAR in asymmetric junctions can account for the observed peak structure, including the feature at $\Delta_1-\Delta_2$.

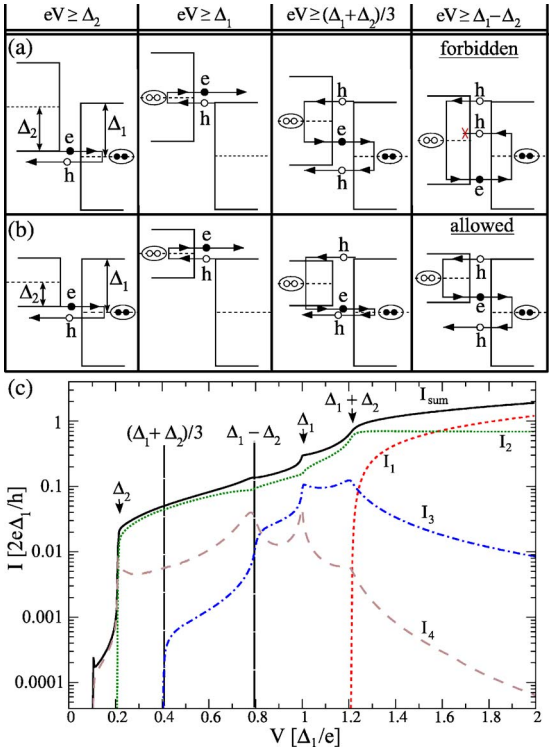

FIG. 4. (Color online) (a), (b) Schematic representation of the most pronounced MARs in asymmetric *SIS* tunnel junctions [(a) $\Delta_2/\Delta_1 \approx 0.8$, (b) $\Delta_2/\Delta_1 \approx 0.4$] and their threshold. (i) At $eV \geqslant \Delta_2$ an electron (e) tunnels from the left SC into the right SC and is reflected into a hole (h) by creating a Cooper pair in the right SC. (ii) At $eV \geqslant \Delta_1$ a hole tunnels from the right SC into the left SC and is reflected into an electron annihilating a Cooper pair in the left SC. (iii) Two-reflection process at $eV \geqslant (\Delta_1+\Delta_2)/3$ involving the tunneling of 3 particles and the creation of a Cooper pair in the right and the annihilation in the left SC. (iv) Special case of the two-reflection process shown in (iii), where the left Andreev reflection takes place just inside the gap of the left SC. This case is only possible in junctions with $\Delta_2/\Delta_1 \leqslant 0.5$. (c) Calculated current contributions I_n to the overall tunneling current I_{sum} (full line) of tunneling processes at nth order in a junction with $\Delta_2/\Delta_1=0.21$ and a transmission coefficient of $\tau=0.2$ at a temperature of 0 K using a full counting statistics calculation. The arrows and the vertical lines mark energies where peaks in the spectrum occur, except at $(\Delta_1+\Delta_2)/3$ (see text).

Similar agreement is obtained for calculations of the temperature dependence shown in Fig. 3(b) by using the measured $\Delta_2(T)$. Better agreement between the calculated lineshapes and those observed experimentally might be obtained by using a model of the tip density of states that accounts for the differences seen in Fig. 3(c). We note that using more than one conduction channel in the calculation did not improve the agreement of the fits.

To learn which MAR processes contribute to the peak at $\Delta_1-\Delta_2$, we use the concept of full counting statistics. As shown in Ref. 18, the total current I_{sum} can be written as a sum of the individual contributions of the different MAR processes $I_{\mathrm{sum}}=\Sigma_n I_n$. Here, I_n is the current contribution of a tunneling process involving the transfer of n electron charges and the occurrence of $n-1$ Andreev reflections, and it can be

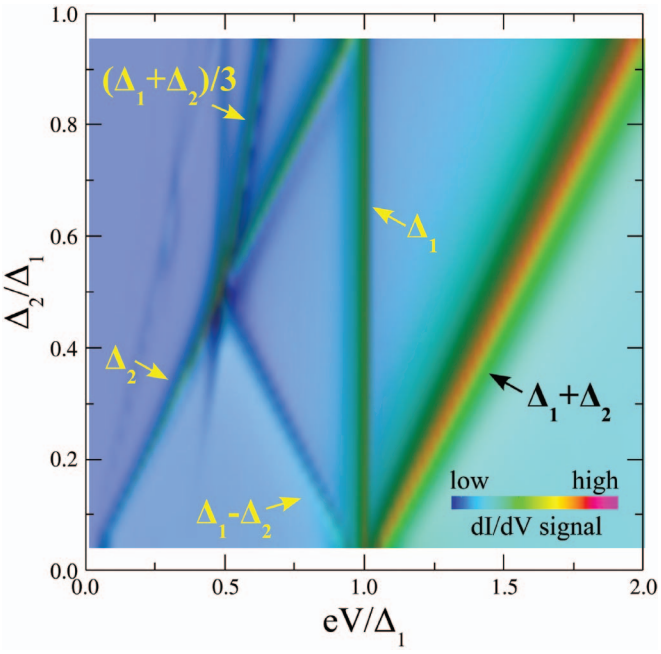

FIG. 5. (Color) Full counting statistics calculation of the dI/dV-signal in an energy range between $0 \leqslant eV \leqslant 2\Delta_1$ between two SC with different gap ratios Δ_2/Δ_1 at a temperature of $T=0$ K and a transmission coefficient of the junction of $\tau=0.25$. The intensity is coded in color (see inset). Peaks at Δ_1, Δ_2, and $\Delta_1+\Delta_2$ are visible for all gap ratios, while the peak at $\Delta_1-\Delta_2$ only exists for a ratio $\Delta_2/\Delta_1 \leqslant 0.5$ and the peak at $(\Delta_1+\Delta_2)/3$ diminishes for a ratio $\Delta_2/\Delta_1 < 0.3$.

expressed as $I_n(V)=\frac{2e}{h}\int_0^{eV} nP_n(V,E)dE$, where $P_n(V,E)$ is the probability of the n-order tunneling process. The MAR probabilities can be obtained by means of a generalization to the asymmetric case of the recipe described in Ref. 18. In Fig. 4(c) we plot the total current and the main contributions I_n for a junction with a gap ratio $\Delta_2/\Delta_1=0.21$. We assume zero temperature and a transmission coefficient of $\tau=0.2$, which corresponds to a junction resistance $R=64.5$ kΩ. The conductance peak at $\Delta_1-\Delta_2$ originates mainly from the large increase of I_3 at this voltage. As illustrated in Fig. 4(b)(iv), such an increase is due to the fact that for $eV \geqslant \Delta_1-\Delta_2$ the two Andreev reflections involved in this MAR process can occur inside the gaps, which implies an enhancement of their probability. Fourth-order processes also contribute strongly to the feature at $\Delta_1-\Delta_2$: the peak in I_4 evident in Fig. 4(c) results in a marked change in the line shape of the dI/dV peak at $\Delta_1-\Delta_2$. So, in short, we propose that the peak at $\Delta_1-\Delta_2$ is due to the enhancement of the probability of a MAR that transfers three electron charges and involves two Andreev reflections.

On the other hand, in contrast to the data shown in Fig. 1, where the ratio between the gaps is nearly equal, none of the I_n shown in Fig. 4(c) produces a significant feature at $(\Delta_1+\Delta_2)/3$. The jump in I_3 is only about $10^{-2}\times I_{\mathrm{sum}}$, because at the onset of this process one of the two Andreev reflections takes place outside the gap, which makes this process quite unlikely [Fig. 4(b)(iii)].

Figure 5 presents in a color coded map the calculated Andreev reflections (dI/dV maxima) for a *SIS* tunnel junc-

tion of transmission coefficient $\tau=0.25$ as a function of normalized junction voltage for gap ratios Δ_2/Δ_1 between 0.05–0.95. At energies of Δ_1, Δ_2, and $\Delta_1+\Delta_2$ Andreev reflections are developed at all ratios. For a ratio $\geqslant 0.3$ a maximum at $(\Delta_1+\Delta_2)/3$ is clearly detectable, while it diminishes for smaller ratios. A maximum at $\Delta_1-\Delta_2$ occurs for all $\Delta_2/\Delta_1 \leqslant 0.5$ and vanishes completely when the gap ratio exceeds 0.5. This calculation is in excellent agreement with our observed spectral features presented in Figs. 1 and 2. For the former with a ratio of $\Delta_2/\Delta_1=0.86$ three peaks inside the gap are located at Δ_1, Δ_2, and $(\Delta_1+\Delta_2)/3$, while the peak at $\Delta_1-\Delta_2$ does not exist. For the latter, we observe the $\Delta_1-\Delta_2$ peak, while the peak at $(\Delta_1+\Delta_2)/3$ is only faintly visible.

To summarize, using a low-temperature STM for the creation and characterization of asymmetric superconducting tunnel junctions we gain new insight into the physics of Andreev reflections by analyzing in detail the observed subgap structure. Especially, for junctions with a relatively small gap ratio Δ_2/Δ_1 we observe peaks at $eV=\pm(\Delta_1-\Delta_2)$, which are not due to the thermal excitation of quasiparticles. All observed subgap features can be understood as Andreev reflections within a full counting statistics model.

M.T. and W.D.S. acknowledge financial support from the Swiss National Science Foundation. J.C.C. was financially supported by the Helmholtz Gemeinschaft. C.P.L. and A.J.H. acknowledge financial support from DARPA.

*Electronic address: Markus.Ternes@epfl.ch

[1] B. N. Taylor and E. Burstein, Phys. Rev. Lett. **10**, 14 (1963).
[2] J. R. Schrieffer and J. W. Wilkins, Phys. Rev. Lett. **10**, 17 (1963).
[3] T. M. Klapwijk, G. E. Blonder, and M. Tinkham, Physica B & C **109**, 1657 (1982).
[4] N. van der Post, E. T. Peters, I. K. Yanson, and J. M. van Ruitenbeek, Phys. Rev. Lett. **73**, 2611 (1994).
[5] E. Scheer, P. Joyez, D. Esteve, C. Urbina, and M. H. Devoret, Phys. Rev. Lett. **78**, 3535 (1997).
[6] E. Scheer, N. Agraït, J. C. Cuevas, A. L. Yeyati, B. Ludoph, A. Martin-Rodero, G. R. Bollinger, J. M. van Ruitenbeek, and C. Urbina, Nature (London) **394**, 154 (1998).
[7] B. Ludoph, N. van der Post, E. N. Bratus, E. V. Bezuglyi, V. S. Shumeiko, G. Wendin, and J. M. van Ruitenbeek, Phys. Rev. B **61**, 8561 (2000).
[8] E. N. Bratus, V. S. Shumeiko, and G. Wendin, Phys. Rev. Lett. **74**, 2110 (1995); D. Averin and A. Bardas, *ibid.* **75**, 1831 (1995).
[9] J. C. Cuevas, A. Martín-Rodero, and A. L. Yeyati, Phys. Rev. B **54**, 7366 (1996).
[10] B. D. Josephson, Phys. Lett. **1**, 251 (1962).
[11] M. Hurd, S. Datta, and P. F. Bagwell, Phys. Rev. B **54**, 6557 (1996); **56**, 11232 (1997).
[12] S. H. Pan, E. W. Hudson, and J. C. Davis, Appl. Phys. Lett. **73**, 2992 (1998).
[13] O. Naaman, W. Teizer, and R. C. Dynes, Phys. Rev. Lett. **87**, 097004 (2001).
[14] J. G. Rodrigo, H. Suderow, and S. Vieira, Eur. Phys. J. B **40**, 483 (2004).
[15] N. Agraït, J. G. Rodrigo, and S. Vieira, Phys. Rev. B **46**, 5814 (1992); O. Naaman and R. C. Dynes, Solid State Commun. **129**, 299 (2004).
[16] Y. Guo, Y.-F. Zhang, X.-Y. Bao, T.-Z. Tang, L.-X. Zhang, W.-G. Zhu, E. G. Wang, Q. Niu, Z. Q. Qiu, J.-F. Jia, Z.-X. Zhao, and Q.-K. Xue, Science **306**, 1915 (2004).
[17] S. Bose, P. Raychaudhuri, R. Banerjee, P. Vasa, and P. Ayyub, Phys. Rev. Lett. **95**, 147003 (2005).
[18] J. C. Cuevas and W. Belzig, Phys. Rev. Lett. **91**, 187001 (2003); J. C. Cuevas and W. Belzig, Phys. Rev. B **70**, 214512 (2004).
[19] A. J. Heinrich, C. P. Lutz, J. A. Gupta, and D. M. Eigler, Science **298**, 1381 (2002).
[20] C. Sürgers, M. Schöck, and H. v. Löhneysen, Surf. Sci. **471**, 209 (2001).
[21] M. Tinkham, *Introduction to Superconductivity* (McGraw-Hill, New York, 1996), p. 77.
[22] R. Rossignoli, J. P. Zagorodny, and N. Canosa, Phys. Lett. A **258**, 188 (1999).
[23] If quasparticle tunneling were the mechanism responsible for the peak at $\Delta_1-\Delta_2$ at low temperatures, then the peak would not diminish at high R, as it does in Fig. 2, and it would appear independently of the gap ratio Δ_1/Δ_2.
[24] Line shapes do not include the supercurrent peak because we include only dissipative current in the calculation. For Figs. 2 and 3 we have used a small imaginary part of the energy $(0.01\Delta_1)$ to simulate the voltage modulation of the experiment.